Spin fractionalization and zero modes in the spin-$\frac{1}{2}$ XXZ chain with boundary fields

Parameshwar R. Pasnoori,[1,2,*] Yicheng Tang,[3] Junhyun Lee,[3] J. H. Pixley,[3,4] Natan Andrei,[3] and Patrick Azaria[5]
[1]Department of Physics, University of Maryland, College Park, Maryland 20742, USA
[2]Laboratory for Physical Sciences, 8050 Greenmead Drive, College Park, Maryland 20740, USA
[3]Department of Physics and Astronomy, Center for Materials Theory, Rutgers University, Piscataway, New Jersey 08854, USA
[4]Center for Computational Quantum Physics, Flatiron Institute, 162 5th Avenue, New York, New York 10010, USA
[5]Laboratoire de Physique Thórique de la Matière Condensée, Sorbonne Université and CNRS, 4 Place Jussieu, 75252 Paris, France

(Received 30 April 2024; revised 1 July 2025; accepted 17 July 2025; published 11 August 2025)

In this work, we argue that the antiferromagnetic spin-$\frac{1}{2}$ XXZ chain in the gapped phase with boundary magnetic fields hosts fractional spin $\frac{1}{4}$ at its edges. Using a combination of Bethe ansatz and the density matrix renormalization group we show that these fractional spins are sharp quantum observables in both the ground and the first excited state as the associated fractional spin operators have zero variance. In the limit of zero edge fields, we argue that these fractional spin operators, once projected onto the low-energy subspace spanned by the ground state and the first excited state, identify with the strong zero-energy mode discovered by Fendley [J. Phys. A: Math. Theor. **49**, 30LT01 (2016)].

DOI: 10.1103/thlq-h58t

I. INTRODUCTION

Since the discovery of solitons carrying half of the electron charge [1,2] it has been widely recognized [3–5] that some states of matter can be characterized by fractional quantum numbers. Maybe the most celebrated example is the fractional quantum Hall state where quasiparticles carry fractional charges [6,7]. Other prominent examples coming from topological phases with short-range topological order, such as symmetry-protected topological (SPT) systems in one dimension, include spin-$\frac{1}{2}$ edge states in the spin-1 Haldane chain [8,9] as well as spin-$\frac{1}{4}$ zero-energy modes (ZEMs) localized at the edges of one-dimensional spin-triplet superconductors [10–12]. In higher dimensions, surface states in topological insulators as well as disordered magnetic systems such as spin ice [13], certain spin liquids [14], and the corners of certain ionic insulators and collinear antiferromagnets [15,16] also exhibit signatures of fractionalization.

Gapped one-dimensional (1D) systems with symmetries can be broadly classified into trivial phases, SPT phases, and symmetry-broken phases [17]. In this respect, to the best of our knowledge, known 1D systems that exhibit fractionalization are SPT phases. In this work, we show that fractionalization also occurs in a system which exhibits a symmetry-broken phase. To this end we shall consider the paradigmatic XXZ spin-$\frac{1}{2}$ chain which exhibits spontaneous symmetry breaking of discrete spin-flip symmetry. We apply magnetic fields at the edges and solve the system exactly with the Bethe ansatz and numerically using the density matrix renormalization group (DMRG) for both even and odd numbers of site chains, and show that in the low-energy sector it hosts quantum spin-$\frac{1}{4}$ states localized at the edges. In the low-energy sector, in addition to the fractionalization of the spin that occurs in the bulk of the chain, where the fundamental spin-1 magnon excitations fractionalize to spin-$\frac{1}{2}$ spinon excitations, there exists further fractionalization where spins $\frac{1}{4}$ are localized at the edges. We shall further argue that these fractional quarter spins are sharp quantum observables. We believe that this result might have some impact on understanding the dynamics [18–24], heat, and spin transport [25–27].

We consider the XXZ Hamiltonian with boundary magnetic fields (h_L, h_R) at the left and the right edges of an open chain,

$$H = \sum_{j=1}^{N-1} \sigma_j^x \sigma_{j+1}^x + \sigma_j^y \sigma_{j+1}^y + \Delta\left(\sigma_j^z \sigma_{j+1}^z - 1\right) + h_L \sigma_1^z + h_R \sigma_N^z, \tag{1}$$

where $\sigma_j^{x,y,z}$ are the Pauli matrices and $\Delta > 1$ is the anisotropy parameter. In the limit where the boundary fields are zero, on top of being $U(1)$ symmetric, (1) is space-parity $\mathbb{P}$ and time-reversal $\mathbb{T}$ invariant. It is also invariant under the $\mathbb{Z}_2 = \{1, \tau\}$ spin-flip symmetry, i.e., $[H, \tau] = 0$ where $\tau = \Pi_1^N \sigma_j^x$. For generic nonzero boundary fields $h_{L,R}, \neq 0$, both $\mathbb{P}$ and $\mathbb{Z}_2$ symmetries are explicitly broken. However, on the two lines $h_L = \pm h_R$ the Hamiltonian (1) displays $\mathbb{P}$ and $\mathbb{P} \circ \mathbb{Z}_2$ symmetries, respectively.

The Hamiltonian in Eq. (1) is integrable by the method of the Bethe ansatz for arbitrary boundary fields $h_{L,R}$ and Δ [28], which is used in the present paper to determine the low-energy eigenstates analytically. The system with periodic boundary conditions was first solved by Bethe [29] in the isotropic limit, $\Delta \to 1$. The solution was later extended to include anisotropy along the z direction [30–35]. In the gapped regime $(\Delta > 1)$ it exhibits a continuous $U(1)$ symmetry and also a discrete $\mathbb{Z}_2$ spin-flip symmetry. The discrete $\mathbb{Z}_2$ symmetry is spontaneously broken [36] and in the thermodynamic limit

*Contact author: pparmesh@umd.edu

the system exhibits two degenerate symmetry-broken ground states [37]. The Bethe ansatz method to include the boundaries was developed in Refs. [38–40] and the ground state and boundary excitations in various bulk phases exhibited by the XXZ spin chain were found in Refs. [41–44]. An independent method to diagonalize the Hamiltonian using vertex operators was developed in Refs. [45,46], and was later extended to include the boundary fields in Ref. [47] where the boundary S matrix and the integral formula for correlation functions have been found. Recently, new band structures in the spectrum at large anisotropies have been found [48]. The system was shown to exhibit a strong zero-energy mode by Fendley [49] and it was recently constructed in Ref. [50] using the algebraic Bethe ansatz.

When $\Delta > 1$ the ground state $|g\rangle$ displays antiferromagnetic (AFM) order with nonzero staggered magnetization $\sigma = \lim_{N\to\infty} N^{-1}\sum_{j=1}^{N}(-1)^j\langle g|\sigma_j^z|g\rangle$ and is gapped. Indeed, for all values of the edge fields, there is a gap (m) in the spectrum to single-particle spin-$\frac{1}{2}$ spinon excitations

$$m = \sinh\gamma\sum_{n\in\mathbb{Z}}\frac{(-1)^n}{\cosh\gamma n}, \qquad \Delta = \cosh\gamma. \tag{2}$$

However, at low fields, i.e., $|h_{L,R}| < \Delta - 1$, the lowest excited state is a *midgap* state $|e\rangle$ which lies below the continuum. We obtain the bound state energies[1] which are given by

$$\begin{aligned} m_\alpha &= h_\alpha + \sinh\gamma\sum_{n\in\mathbb{Z}}(-1)^n\frac{\sinh(\gamma\tilde{\epsilon}_\alpha|n|)}{\cosh\gamma n}e^{-\gamma|n|},\\ h_\alpha &= -\sinh\gamma\tanh\left(\frac{\tilde{\epsilon}_\alpha\gamma}{2}\right),\\ \tilde{\epsilon}_\alpha &= -\frac{2}{\gamma}\text{arctanh}\left(\frac{h_\alpha}{\sinh\gamma}\right), \end{aligned} \tag{3}$$

where $\alpha = (L, R)$. This midgap state is reminiscent of the existence of spin-$\frac{1}{2}$ boundary bound states, localized at the left and the right edges. The spin quantum numbers and energies of the ground state as well as the midgap state depend on both the parity of the number of sites, $(-1)^N$, as well as on the boundary fields $h_{L,R}$. When N is odd, the two states $|g\rangle$ and $|e\rangle$ have opposite total spins $S^z = \pm 1/2$. Taking as a reference state the $|-\frac{1}{2}\rangle$ state with energy E_0, the $|+\frac{1}{2}\rangle$ state is obtained by adding a localized bound state at each *edge*. This state has energy $E_0 + m_L + m_R$. Depending on the edge magnetic fields, and hence on the sign of $m_L + m_R$, the ground state and the midgap state $(|g\rangle, |e\rangle)$ are $(|-\frac{1}{2}\rangle, |+\frac{1}{2}\rangle)$ when $h_L + h_R > 0$ and $(|\frac{1}{2}\rangle, |-\frac{1}{2}\rangle)$ when $h_L + h_R < 0$. Notice that on the line $h_L + h_R = 0$, the two states $|\pm\frac{1}{2}\rangle$ are degenerate. In the $N \to \infty$ limit, there is spontaneous symmetry breaking (SSB) of the $\mathbb{P}\circ\mathbb{Z}_2$ symmetry. In the particular case of zero edge fields, both $\mathbb{P}$ and $\mathbb{Z}_2$ symmetries are spontaneously broken. For N even both $(|g\rangle, |e\rangle)$ states have total spins $S^z = 0$ and the bound state construction is presented in the Supplemental Material (SM) [51]. We display in Fig. 1 the phase diagram for low fields for an odd number of sites N.

[1]Note that a different expression was obtained in [42,43]. We also use the same notation as in [43].

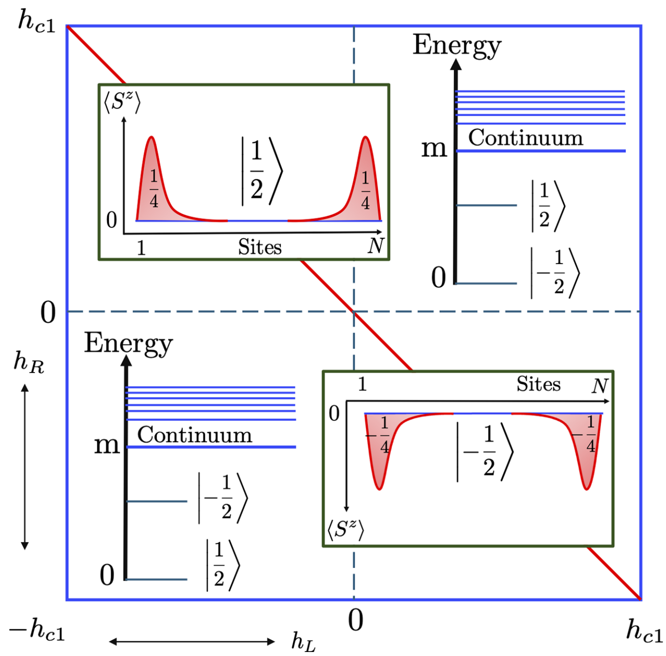

FIG. 1. Ground state phase diagram of the XXZ model with edge fields smaller than the critical field $|h_{L,R}| < h_c = \Delta - 1$ and for an odd number of sites. In each of the two phases separated by the line $h_L + h_R = 0$ we show the ground state as well as the first excited state which is a midgap state below the continuum. Both states host fractional quarter spins $\mathcal{S}_{L,R} = \pm 1/4$ at both edges of the chain. These fractional spins are sharp quantum observables which reconstruct the total spin of each state $S^z = \mathcal{S}_L + \mathcal{S}_R = \pm 1/2$. The insets depict the $\pm 1/4$ quarter spins by exponentially localized accumulations at the boundaries shown in red color in both the $|\pm\frac{1}{2}\rangle$ states. On the separatrix $h_L + h_R = 0$ there is spontaneous symmetry breaking and the edge spin operator becomes a zero-energy mode.

II. SPIN PROFILES

Due to the open boundaries and the presence of the edge fields (h_L, h_R), the spin profiles $S_j^z = \langle\sigma_j^z\rangle/2$ in both the ground state and the midgap state differ from the bulk antiferromagnetic order close to the boundaries. The Bethe ansatz results suggest that for large enough N we may write (see SM [51] for more details)

$$S_j^z = (-1)^j\frac{\sigma}{2} + \Delta S^z(j), \tag{4}$$

where

$$\sigma = \pm\left[\Pi_{n=1}^{\infty}\left(\frac{1-q^{2n}}{1+q^{2n}}\right)\right]^2, \quad q = e^{-\gamma}, \tag{5}$$

is the exact staggered magnetization of the XXZ chain in the thermodynamic limit and $\Delta S^z(j)$ is the relative deviation with respect to the anitferromagnetic (AFM) bulk profile. Due to the gap in the bulk these deviations are expected to be localized close to both the left and the right edges

$$\Delta S^z(j) = \Delta S_L^z(j) + \Delta S_R^z(j), \tag{6}$$

where $\Delta S_{L,R}^z(j)$ are localized close to $j = 1$ and $j = N$, respectively [i.e., $\Delta S_{L,R}^z(N/2) \sim e^{-N/2}$]. This is indeed what we find, where we clearly observe an exponential localization of the relative spin accumulation for various values of Δ at constant boundary fields $h_L = h_R = 0.2$ (see SM [51]).

III. SPIN FRACTIONALIZATION

The spin accumulations, or depletions, do not come as a surprise and are expected due to the open boundaries and the presence of the edge fields. What is nontrivial is that they correspond to a genuine spin fractionalization in both the ground state and the midgap state. As we shall now demonstrate, in the thermodynamic limit and for all $\Delta > 1, h_{L,R}$, there exist fractionalized quarter spin operators associated with each edge, $\hat{\mathcal{S}}^z_L$ and $\hat{\mathcal{S}}^z_R$, which have well-defined fractional eigenvalues

$$\hat{\mathcal{S}}^z_{L,R}|g(e)\rangle = \mathcal{S}^z_{L,R}|g(e)\rangle, \quad \mathcal{S}^z_{L,R} = \pm\tfrac{1}{4}. \tag{7}$$

In the basis $(|g\rangle, |e\rangle)$ the above fractional spin operators commute with each other, and anticommute with the spin-flip operator, i.e., $[\hat{\mathcal{S}}^z_L, \hat{\mathcal{S}}^z_R] = 0$, $\{\tau, \hat{\mathcal{S}}^z_{L,R}\} = 0$. Together, they reconstruct the z component of the total spin $\hat{S}^z = \sum_{i=1}^N \hat{S}^z_i$, namely

$$\hat{S}^z = \hat{\mathcal{S}}^z_L + \hat{\mathcal{S}}^z_R. \tag{8}$$

Since the edge spin operators have fractional spin $\pm 1/4$ one may verify that the $\hat{S}^z$ have eigenvalues 0 or $\pm 1/2$ depending on whether N is even or odd. For the fractional spin operators (7) to describe sharp quantum observables in the subspace spanned by $(|g\rangle, |e\rangle)$, not only do they have to average to $\pm 1/4$ in both states, but also their variance must vanish in the thermodynamic limit, i.e.,

$$\langle \hat{\mathcal{S}}^z_{L,R}\rangle = \mathcal{S}_{L,R}, \tag{9}$$

and

$$\delta\mathcal{S}^2_{L,R} \equiv \langle (\hat{\mathcal{S}}^z_{L,R})^2\rangle - (\mathcal{S}_{L,R})^2 = 0, \tag{10}$$

where the average $\langle \cdots \rangle$ is taken in each of the two states ($|g\rangle$ and $|e\rangle$).

Following the authors of Refs. [4,5] we define the fractional spin operators as their convolution with a decaying function $f(x)$, where we take $f(x) = e^{-\alpha x}$ to write

$$\hat{\mathcal{S}}^z_L = \lim_{\alpha\to 0}\lim_{N\to\infty}\sum_{j=1}^N f(j)\frac{\sigma^z_j}{2}, \tag{11}$$

$$\hat{\mathcal{S}}^z_R = \lim_{\alpha\to 0}\lim_{N\to\infty}\sum_{j=1}^N f(N+1-j)\frac{\sigma^z_j}{2}, \tag{12}$$

which takes the limit $\alpha \to 0$ after the limit $N \to \infty$. We stress that the order of limits in (12) is important since by taking the limit $\alpha \to 0$ first, both $\mathcal{S}^z_{L,R}$ would identify with the total magnetization S^z.

Due to the AFM long-range order it is convenient to distinguish between the contributions of the staggered part of the spin profile and that of the exponentially localized contributions,

$$\hat{\mathcal{S}}^z_L = -\frac{\sigma}{4} + \Delta\hat{\mathcal{S}}^z_L, \quad \hat{\mathcal{S}}^z_R = -\frac{\sigma}{4}(-1)^N + \Delta\hat{\mathcal{S}}^z_R, \tag{13}$$

where the relative accumulation operators are given by

$$\Delta\hat{\mathcal{S}}^z_L = \lim_{\alpha\to 0}\lim_{N\to\infty}\frac{1}{2}\sum_{j=1}^N \left[\sigma^z_j - \sigma(-1)^j\right]e^{-\alpha j},$$

$$\Delta\hat{\mathcal{S}}^z_R = \lim_{\alpha\to 0}\lim_{N\to\infty}\frac{1}{2}\sum_{j=1}^N \left[\sigma^z_j - \sigma(-1)^j\right]e^{-\alpha(N+1-j)}. \tag{14}$$

We have used the identity $\lim_{\alpha\to 0}\sum_{j=1}^\infty (-1)^j e^{-\alpha j} = -\frac{1}{2}$. In practice, one may set $\alpha = 0$ in (14) provided the summation over j extends to the middle of the chain $j_{\max} = N/2$. Convergence is then expected to be of order $e^{-N/2}$. Before going further, it is worthy to point out that although the relative accumulations defined in Eq. (14) have the same variance as the fractional spin operators (12) they do not qualify as spin operators in the sense that they do not anticommute with the spin-flip operator τ, i.e., $\{\Delta\hat{\mathcal{S}}_{L,R}, \tau\} \neq 0$.[2] These relative accumulations would have fractional eigenvalues which depend on the anisotropy parameter Δ. Taking into account the AFM long-range order in the bulk is essential for the spin accumulations to have fractional eigenvalues $\pm 1/4$ independently of the model parameters, as we shall see.

IV. SPIN-$\pm\frac{1}{4}$ ACCUMULATIONS

Evaluating (14) would require the knowledge of the wave function of the ground state and the midgap states which is a formidable task within the Bethe ansatz approach. Hence, we resort to the complementary DMRG approach which is implemented through the TENPY software [52], that allows access to the ground state and midgap state with arbitrary precision owing to the gapped nature of both of these states. We take a maximum bond dimension of 400, with a minimal singular value decomposition cutoff of 10^{-10}, and converge the energy up to a maximal energy error on the order of $\sim 10^{-10}$. We have computed the edge spin accumulations $\mathcal{S}_L = \langle \hat{\mathcal{S}}^z_L\rangle$ and $\mathcal{S}_R = \langle \hat{\mathcal{S}}^z_R\rangle$ in both the ground state and the midgap state for a wide range of boundary fields $|h_{L,R}| < \Delta - 1$ and parameters $\Delta > 1$.

All together our results are consistent with an accumulation of a spin $\mathcal{S}_{L,R} = \pm 1/4$ at the two edges of the system in both the ground state and the midgap state. Furthermore, we verify explicitly that these quarter spins reconstruct the total spin S^z, as given by Eq. (8), of the ground state and the midgap state for both N even and N odd. We show here our results for an odd number of sites fixing $\Delta = 3$ and an anisotropic edge field configuration $h_L = 0$ with varying h_R in Fig. 2. To check that the quarter spins observed so far do not depend on the value of $\Delta > 1$, we also show the spin accumulations fixing $h_L = h_R = 0.2$ (in this case $\mathcal{S}_L = \mathcal{S}_R$ owing to the $\mathbb{P}$ symmetry) and varying Δ. More results are given in the SM [51].

V. VARIANCE

We also calculated the spin variance to directly verify that the quarter spins found so far are sharp quantum observables.

[2] For instance it would not couple to an external magnetic field penetrating smoothly near the left edge whereas $\hat{\mathcal{S}}_L$ would.

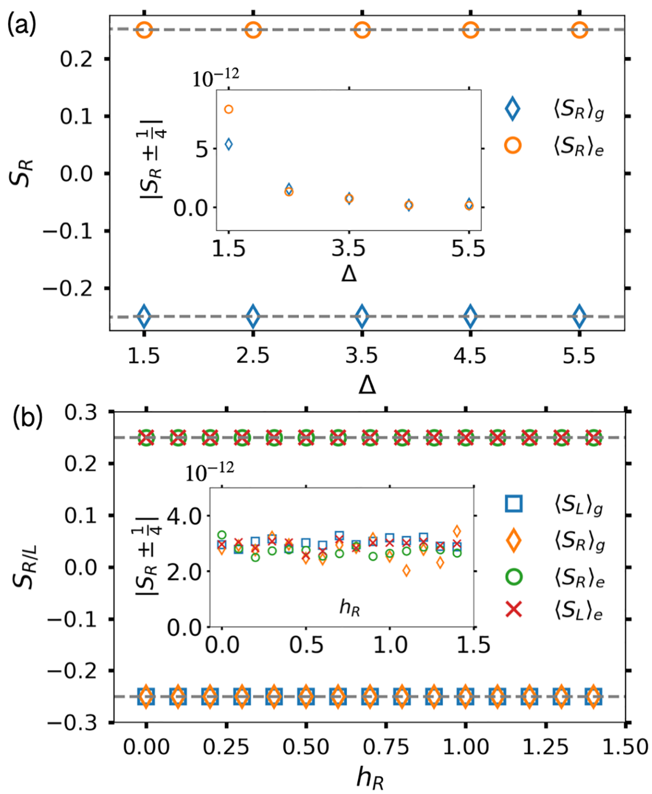

FIG. 2. Edge spin accumulation $\mathcal{S}_{L/R} = \langle \hat{\mathcal{S}}^z_{L/R}\rangle$ in the ground state $|g\rangle$, with total spin $S^z = -\frac{1}{2}$, and in the midgap state $|e\rangle$, with total spin $S^z = \frac{1}{2}$. The model parameters used are (a) $N = 1001$, $h_R = h_L = 0.2$ with varying Δ, and (b) $N = 1001$, $h_L = 0$, and $\Delta = 3$ with varying h_R. The dashed gray lines are on the curve $S = \pm 1/4$ to represent the expected value. Insets show the difference of numerical values from the expected value, which is on the order of the DMRG accuracy $\sim 10^{-12}$.

In the thermodynamic limit, the variance, as defined in Eq. (10), is then obtained as

$$\delta S^2_L \equiv \lim_{\alpha\to 0}\lim_{N\to\infty} \delta S^2(N,\alpha). \tag{15}$$

Taking the $N \to \infty$ is challenging and we circumvent this issue by assuming an ansatz relating $\delta S^2_L(N,\alpha)$ and $\delta S^2_L(\infty,\alpha)$,

$$\delta S^2_L(N,\alpha) = \delta S^2(\infty,\alpha) - \frac{A}{\Delta}\alpha e^{-B\alpha N}. \tag{16}$$

We have verified this ansatz by taking the difference of $\delta S^2_L(N,\alpha)$ for different N's. This is shown in Fig. 3. The fitted parameter $B \approx 2$ is nearly independent of the boundary fields, while A takes a nonuniversal value. With the above ansatz we can calculate δS^2_L without explicitly taking the thermodynamic limit yielding $\delta S^2_L = 0$ and hence find that the variance in Eq. (10) vanishes.

In summary we find that in the low-energy subspace spanned by the ground state $|g\rangle$ and the midgap state $|e\rangle$ one can assign to the left and the right edges a fractional spin state with eigenvalues $\mathcal{S}_{L,R} = \pm\frac{1}{4}$. On the basis of our results we find it safe to expect that this is to be the case irrespective of the anisotropy parameter $\Delta > 1$ and the values of the edge fields $[h_{L,R}| < \Delta - 1$. Due to the zero variance of

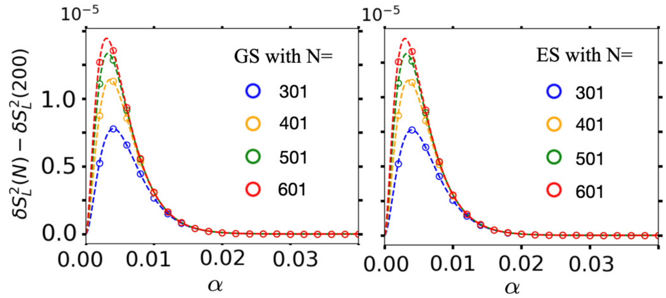

FIG. 3. Edge spin variance $\delta S^2_L(N,\alpha)$ in (left) the ground state (GS) $S^z = -\frac{1}{2}$ and (right) the midgap state (ES) $S^z = \frac{1}{2}$ with model parameters $\Delta = 3$, $h_L = h_R = 0.2$, and varying N.

the fractional spin operators (12), the quarter spins $\mathcal{S}_{L,R}$ are not simple quantum averages of half-integer spins at different sites but rather sharp quantum observables. The orientations of these quarter spins depend on the boundary fields and on the parity of the number of sites N in such a way that (8) is satisfied in all ground states. Since the fractional spins at each edge are good quantum numbers we may then label the ground state and the midgap state as $|g(e)\rangle = |\mathcal{S}_L, \mathcal{S}_R\rangle$. For odd N spin chains these states are given by $|\pm 1/4, \pm 1/4\rangle$ whereas for even chains they are given by $|\pm 1/4, \mp 1/4\rangle$. One can easily verify that the total spin is $S^z = \pm 1/2$ and $S^z = 0$ for the odd and even cases. We want to point out that the existence of a gap above the ground state and the midgap state seems to be crucial for the quarter spins to be sharp quantum observables, and hence fractional spins $\pm 1/4$ only exist in the low-energy states which are separated from the continuum. Indeed, in the limit $\Delta \to 1$ where the mass gap goes to zero, we end up with the XXX Heisenberg chain. In this case it was found in Ref. [53] that although the fractional spins $\pm 1/4$ exist in the ground state, their variance is not zero and hence the fractional spins are not genuine quantum observables.

VI. DISCUSSION

The first natural question that arises is whether or not the quarter spins found so far survive in the higher excited states of the spectrum of the XXZ chain. However, excited states above the midgap state contain propagating spinons. In such case, even if a quarter spin can be defined *on average*, we do not expect its variance to be zero as found for the XXX spin chain with edge fields [53]. Another related question is whether these quarter spins survive edge fields higher than the critical value $h_c = \Delta - 1$. In this regime there are no midgap states [41–44] but we believe that sharp quarter spins exist in the ground state due to the existence of the spectral gap.

We shall end by commenting about the relation between the quarter spins found in this work with spontaneous symmetry breaking of the $\mathbb{Z}_2$ symmetry in the case of zero edge fields, i.e., $h_L = h_R = 0$. In the limit of zero edge fields the two states $|g(e)\rangle$ become degenerate in the thermodynamic limit as the bound state energies (3) vanish. Without loss of generality one may then choose $|g\rangle = |-1/4, -1/4\rangle$ for N odd and $|g\rangle = |1/4, -1/4\rangle$ for N even. The two linear combinations

$|\pm\rangle = (|g\rangle \pm |e\rangle)/\sqrt{2}$ are eigenstates of τ, i.e., $\tau|\pm\rangle = \pm|\pm\rangle$. Since, in the same limit each of the two states $|g(e)\rangle$ are eigenstates of $\hat{S}^z_{L,R}$, the fractional spin operators map the two states $|\pm\rangle$ onto each other, i.e., $\hat{S}^z_{L,R}|\pm\rangle = (-1)^N \frac{1}{4}|\mp\rangle$. Hence the fractional spin operators are zero-energy modes (ZEMs) in the basis $|g\rangle$ and $|e\rangle$. Notice that, since in this subspace $\hat{S}^z_{L,R}$ is not independent as $\hat{S}^z_L = \pm\hat{S}^z_R$ in both states, there exists only one ZEM, say $\hat{S}^z_L$. At this point it is worth mentioning that the Hamiltonian (1) displays the remarkable property, discovered by Fendley [49], of having a strong zero-energy mode Ψ_F in the thermodynamic limit satisfying the following properties,

$$[\Psi_F, H] = 0, \quad \{\Psi_F, \tau\} = 0, \quad \Psi_F^2 = 1. \tag{17}$$

The existence of the latter operator ensures that in the $N \to \infty$ limit the Hilbert space associated with the XXZ spin chain fractionalizes into two degenerated towers with eigenvalues $\tau = \pm 1$ which are mapped onto each other by the action of Ψ_F. We may therefore conclude that when *projected* in the low-energy subspace spanned by the ground state and the midgap state the Fendley operator identifies with the fractional spin operator

$$\Psi_F \equiv 4\hat{S}^z_L. \tag{18}$$

Of course, since we do not expect a quarter fractional spin to be sharp in all the excited states, $\hat{S}^z_L$ is not a strong ZEM in contrast with the Fendley operator Ψ_F, but rather a *soft* ZEM. We finally notice that, following the same lines of arguments as given above, the fractional spin $\hat{S}^z_L$ is also a soft ZEM on the two lines $h_L = h_R$ for N even and $h_L = -h_R$ for N odd where the symmetries $\mathbb{P} \circ \mathbb{Z}_2$ and $\mathbb{P}$ are spontaneously broken. It would be interesting to know if a strong zero mode similar to (17) exists on these two symmetric lines. We hope that the quarter spins found in this work could be probed in experiments using ultracold atoms in optical lattices [54] and Josephson junction arrays [55].

ACKNOWLEDGMENTS

This work is is partially supported by the Air Force Office of Scientific Research under Grant No. FA9550-20-1-0136 (J.L., J.H.P.), NSF Career Grant No. DMR-1941569 (J.H.P.), and the Alfred P. Sloan Foundation through a Sloan Research Fellowship (J.H.P.).

[1] R. Jackiw and C. Rebbi, Soliton with fermion number 1/2, Phys. Rev. D **13**, 3398 (1976).
[2] W. P. Su, J. R. Schriefer, and A. J. Hegger, Soliton in polyacetylene, Phys. Rev. Lett. **42**, 1698 (1979).
[3] J. Goldstone and F. Wilczek, Fractional quantum numbers on solitons, Phys. Rev. Lett. **47**, 986 (1981).
[4] S. Kivelson and J. R. Schriefer, Fractional charge, a sharp quantum observable, Phys. Rev. B **25**, 6447 (1982).
[5] R. Jackiw, A. K. Kerman, I. Klebanov, and G. Semenoff, Fluctuations of fractional charge in soliton anti-soliton systems, Nucl. Phys. B **225**, 233 (1983).
[6] R. B. Laughlin, Anomalous quantum Hall effect: An incompressible quantum fluid with fractionally charged excitations, Phys. Rev. Lett. **50**, 1395 (1983).
[7] D. C. Tsui, H. L. Stormer, and A. C. Gossard, Two-dimensional magnetotransport in the extreme quantum limit, Phys. Rev. Lett. **48**, 1559 (1982).
[8] F. D. M. Haldane, Continuum dynamics of the 1-D Heisenberg antiferromagnet: Identification with the O(3) nonlinear sigma model, Phys. Lett. A **93**, 464 (1983).
[9] I. Affleck, T. Kennedy, E. H. Lieb, and H. Tasaki, Rigorous results on valence-bond ground states in antiferromagnets, Phys. Rev. Lett. **59**, 799 (1987).
[10] A. Keselman and E. Berg, Gapless symmetry-protected topological phase of fermions in one dimension, Phys. Rev. B **91**, 235309 (2015).
[11] P. R. Pasnoori, N. Andrei, and P. Azaria, Edge modes in one-dimensional topological charge conserving spin-triplet superconductors: Exact results from Bethe ansatz, Phys. Rev. B **102**, 214511 (2020).
[12] P. R. Pasnoori, N. Andrei, and P. Azaria, Boundary-induced topological and mid-gap states in charge conserving one-dimensional superconductors: Fractionalization transition, Phys. Rev. B **104**, 134519 (2021).
[13] C. Castelnovo, R. Moessner, and S. L. Sondhi, Spin ice, fractionalization, and topological order, Annu. Rev. Condens. Matter Phys. **3**, 35 (2012).
[14] A. Banerjee, C. A. Bridges, J. Q. Yan, A. A. Aczel, L. Li, M. B. Stone, G. E. Granroth, M. D. Lumsden, Y. Yiu, J. Knolle, S. Bhattacharjee, D. L. Kovrizhin, R. Moessner, D. A. Tennant, D. G. Mandrus, and S. E. Nagler, Proximate Kitaev quantum spin liquid behaviour in a honeycomb magnet, Nat. Mater. **15**, 733 (2016).
[15] H. Watanabe and H. C. Po, Fractional corner charge of sodium chloride, Phys. Rev. X **11**, 041064 (2021).
[16] H. Watanabe, Y. Kato, H. C. Po, and Y. Motome, Fractional corner magnetization of collinear antiferromagnets, Phys. Rev. B **103**, 134430 (2021).
[17] X. Chen, Z.-C. Gu, and X.-G. Wen, Classification of gapped symmetric phases in one-dimensional spin systems, Phys. Rev. B **83**, 035107 (2011).
[18] W. Liu and N. Andrei, Quench dynamics of the anisotropic Heisenberg model, Phys. Rev. Lett. **112**, 257204 (2014).
[19] J. Lancaster and A. Mitra, Quantum quenches in an *XXZ* spin chain from a spatially inhomogeneous initial state, Phys. Rev. E **81**, 061134 (2010).
[20] B. Pozsgay, M. Mestyan, M. A. Werner, M. Kormos, G. Zarand, and G. Takacs, Correlations after quantum quenches in the *XXZ* spin chain: Failure of the generalized Gibbs ensemble, Phys. Rev. Lett. **113**, 117203 (2014).
[21] M. Mestyán, B. Pozsgay, G. Takács, and M. A. Werner, Quenching the XXZ spin chain: quench action approach versus generalized Gibbs ensemble, J. Stat. Mech. (2015) P04001.

[22] M. S. Foster, T. C. Berkelbach, D. R. Reichman, and E. A. Yuzbashyan, Quantum quench spectroscopy of a Luttinger liquid: Ultrarelativistic density wave dynamics due to fractionalization in an XXZ chain, Phys. Rev. B **84**, 085146 (2011).

[23] K. Joel, D. Kollmar, and L. F. Santos, An introduction to the spectrum, symmetries, and dynamics of spin-1/2 Heisenberg chains, Am. J. Phys. **81**, 450 (2013).

[24] G. Misguich, K. Mallick, and P. L. Krapivsky, Dynamics of the spin-$\frac{1}{2}$ Heisenberg chain initialized in a domain-wall state, Phys. Rev. B **96**, 195151 (2017).

[25] B. Bertini, M. Collura, J. De Nardis, and M. Fagotti, Transport in out-of-equilibrium XXZ chains: Exact profiles of charges and currents, Phys. Rev. Lett. **117**, 207201 (2016).

[26] A. De Luca, M. Collura, and J. De Nardis, Nonequilibrium spin transport in integrable spin chains: Persistent currents and emergence of magnetic domains, Phys. Rev. B **96**, 020403(R) (2017).

[27] V. B. Bulchandani, R. Vasseur, C. Karrasch, and J. E. Moore, Bethe-Boltzmann hydrodynamics and spin transport in the XXZ chain, Phys. Rev. B **97**, 045407 (2018).

[28] Y. Wang, W.-L. Yang, J. Cao, and K. Shi, *Off-Diagonal Bethe Ansatz for Exactly Solvable Models* (Springer, Berlin, 2015).

[29] H. Bethe, Zur Theorie der Metalle, Z. Phys. **71**, 205 (1931).

[30] R. Orbach, Linear antiferromagnetic chain with anisotropic coupling, Phys. Rev. **112**, 309 (1958).

[31] L. R. Walker, Antiferromagnetic linear chain, Phys. Rev. **116**, 1089 (1959).

[32] C. N. Yang and C. P. Yang, One-dimensional chain of anisotropic spin-spin interactions. I. Proof of Bethe's hypothesis for ground state in a finite system, Phys. Rev. **150**, 321 (1966).

[33] C. N. Yang and C. P. Yang, One-dimensional chain of anisotropic spin-spin interactions. II. Properties of the ground-state energy per lattice site for an infinite system, Phys. Rev. **150**, 327 (1966).

[34] C. N. Yang and C. P. Yang, One-dimensional chain of anisotropic spin-spin interactions. III. Applications, Phys. Rev. **151**, 258 (1966).

[35] O. Babelon, H. J. de Vega, and C. M. Viallet, Analysis of the Bethe ansatz equations of the *XXZ* model, Nucl. Phys. B **220**, 13 (1983).

[36] O. F. Syljuåsen, Entanglement and spontaneous symmetry breaking in quantum spin models, Phys. Rev. A **68**, 060301(R) (2003).

[37] M. Takahashi, *Thermodynamics of One-Dimensional Solvable Models* (Cambridge University Press, Cambridge, UK, 1999).

[38] F. C. Alcaraz, M. N. Barber, M. T. Batchelor, R. J. Baxter, and G. R. W. Quispel, Surface exponents of the quantum XXZ, Ashkin-Teller and Potts models, J. Phys. A: Math. Gen. **20**, 6397 (1987).

[39] I. V. Cherednik, Factorizing particles on a half-line and root systems, Theor. Math. Phys. **61**, 977 (1984).

[40] E. K. Sklyanin, Boundary conditions for integrable quantum systems, J. Phys. A: Math. Gen. **21**, 2375 (1988).

[41] S. Skorik and H. Saleur, Boundary bound states and boundary bootstrap in the sine-Gordon model with Dirichlet boundary conditions, J. Phys. A: Math. Gen. **28**, 6605 (1995).

[42] A. Kapustin and S. Skorik, Surface excitations and surface energy of the antiferromagnetic XXZ chain by the Bethe ansatz approach, J. Phys. A: Math. Gen. **29**, 1629 (1996).

[43] S. Grijalva, J. Nardis, and V. Terras, Open XXZ chain and boundary modes at zero temperature, SciPost Phys. **7**, 023 (2019).

[44] T. Nassar and O. Tirkkonen, Excited states in the twisted XXZ spin chain, J. Phys. A: Math. Gen. **31**, 9983 (1998).

[45] B. Davies, O. Foda, M. Jimbo, T. Miwa, and A. Nakayashiki, Diagonalization of the XXZ Hamiltonian by vertex operators, Commun. Math. Phys. **151**, 89 (1993).

[46] M. Jimbo, K. Miki, T. Miwa, and A. Nakayashiki, Correlation functions of the XXZ model for $\Delta < 1$, Phys. Lett. A **168**, 256 (1992).

[47] M. Jimbo, R. Kedem, T. Kojima, H. Konno, and T. Miwa, XXZ chain with a boundary, Nucl. Phys. B **441**, 437 (1995).

[48] A. Sharma and M. Haque, Fine structures in the spectrum of the open-boundary Heisenberg chain at large anisotropies, Phys. Rev. A **89**, 043608 (2014).

[49] P. Fendley, Strong zero modes and eigenstate phase transitions in the XYZ/interacting Majorana chain, J. Phys. A: Math. Theor. **49**, 30LT01 (2016).

[50] E. Vernier, H.-C. Yeh, L. Piroli, and A. Mitra, Strong zero modes in integrable quantum circuits, Phys. Rev. Lett. **133**, 050606 (2024).

[51] See Supplemental Material at http://link.aps.org/supplemental/10.1103/thlq-h58t for the Bethe ansatz solution where we obtain the ground states and low energy excitations. Using these Bethe ansatz results we obtain the ansatz for the magnetization profile in the low energy states, which is then analyzed numerically using DMRG.

[52] J. Hauschild and F. Pollmann, Efficient numerical simulations withtensor networks: Tensor Network Python (TeNPy), SciPost Phys. Lect. Notes 5 (2018).

[53] P. R. Pasnoori, J. Lee, J. H. Pixley, N. Andrei, and P. Azaria, Boundary quantum phase transitions in the spin-$\frac{1}{2}$ Heisenberg chain with boundary magnetic fields, Phys. Rev. B **107**, 224412 (2023).

[54] L.-M. Duan, E. Demler, and M. D. Lukin, Controlling spin exchange interactions of ultracold atoms in optical lattices, Phys. Rev. Lett. **91**, 090402 (2003).

[55] L. I. Glazman and A. I. Larkin, New quantum phase in a one-dimensional Josephson array, Phys. Rev. Lett. **79**, 3736 (1997).